JOURNAL OF MATERIALS SCIENCE 31 (1996) 1603–1608

Effect of Al_2O_3 addition on phase reaction of the AlN–Y_2O_3 system

N. H. KIM, K. KOMEYA, T. MEGURO
Department of Materials Chemistry, Yokohama National University, 156 Tokiwadai, Hodogayaku, Yokohama 240, Japan

It is well known that the existence of oxygen in the sintering of aluminium nitride (AlN) causes the degradation of thermal conductivity. To clarify the role of the oxygen, the effect of Al_2O_3 addition on the phase reaction of the AlN–Y_2O_3 system at high temperatures of 1900 and 1950 °C was investigated. In the AlN–Al_2O_3 system, γ-AlON and 27R polytypoid were formed at 1900 and 1950 °C, respectively, and the ratio of each crystal increased with increasing Al_2O_3 content. The resultant phase was found to be in agreement with the phase diagram given by McCauley and Corbin. In the AlN–Y_2O_3 system, YAM phase or YAM plus unreacted Y_2O_3 were identified. Phase reaction in the AlN–Al_2O_3–$2Y_2O_3$ system was quite different from that of the AlN–Al_2O_3 system: namely, γ-AlON and 27R coexisted even at 1950 °C, which is inconsistent with McCauley and Corbin's diagram. It was confirmed by the dilatometric method and phase reaction data using some couples, that Al_2O_3 strongly affected the phase reaction in the AlN–Y_2O_3 system, indicating that the shrinkage of the Al_2O_3-doped specimen was initiated at somewhat lower temperatures. The grain morphology depended on the phase changes shown above, in which AlN and γ-AlON were granular, and 27R polytypoid was plate-like.

1. Introduction

Aluminium nitride (AlN) has attracted much attention as a high thermal conductive and electrical insulative material for electronic substrates and packages. The thermal conductivity of AlN ceramics, which has been theoretically predicted to be 320 $W m^{-1} K^{-1}$ at room temperature [1], is strongly influenced by its chemical purity and density. In general, AlN is densified using typical sintering aids, such as rare-earth compounds (Y_2O_3, YF_3) [2, 3] and alkaline earth compounds (CaO, $CaCO_3$) [4, 5] because of its poor sinterability due to the covalent bond structure.

In most cases, AlN raw powder contains a small amount of oxygen which forms Al_2O_3 on the surface and substitutes in the nitrogen lattice in the bulk. It is known that the thermal properties of AlN ceramics are especially affected by the coexisting oxygen [1], and that a small amount of oxygen may play a significant role in the densification of Y_2O_3-containing components. Incidentally, the formation of various aluminates, polytypoids, and spinels has been recognized in the reaction of AlN and Y_2O_3 with coexisting oxygen. Therefore, the content of oxygen as Al_2O_3 results in the structural changes corresponding to the ratio of AlN/Al_2O_3.

Yamaguchi and Yanagida [6], Long and Foster [7], and Adams *et al.* [8] have reported the phase relation regarding the formation of spinel-type AlON through reaction of AlN with Al_2O_3. Sakai [9] and McCauley and Corbin [10, 11] have also proposed a phase diagram in the AlN–Al_2O_3 system, indicating the formation of spinels and polytypoids corresponding to the amount of coexisting oxygen. Komeya *et al.* [12], Gauckler *et al.* [13], and Jack [14] have reported the formation of polytypoids in the Si–Al–O–N system, and Jack [14], Sakai [9], and McCauley and Corbin [11] have examined the formation of several polytypoids in the system Al–O–N.

Through these studies, the phase reaction in a binary system has been clarified. However, to date there is little information on the ternary AlN–Al_2O_3-sintering additives system [15].

In the present work, the effect of Al_2O_3 addition on the phase reaction of the AlN–Y_2O_3 system at high temperatures was investigated.

2. Experimental procedure

2.1. Raw materials

Commercially available AlN powder (Tokuyama Co. Ltd) and Al_2O_3 powder (Sumitomo Chemical Co. Ltd), with average particle sizes of approximately 0.6 and 0.4 μm, respectively, were used in this study. AlN raw powder contained about 500 p.p.m. total cation impurities and 0.8 wt % oxygen. Y_2O_3 powder (Mitsubishi Chemical Ind. Ltd, average particle size < 1 μm (78%)) as a sintering aid was added to the AlN raw powder. The amounts of Al_2O_3 and Y_2O_3 were adjusted in the range of 0–30 and 0–10 wt %, respectively.

0022-2461

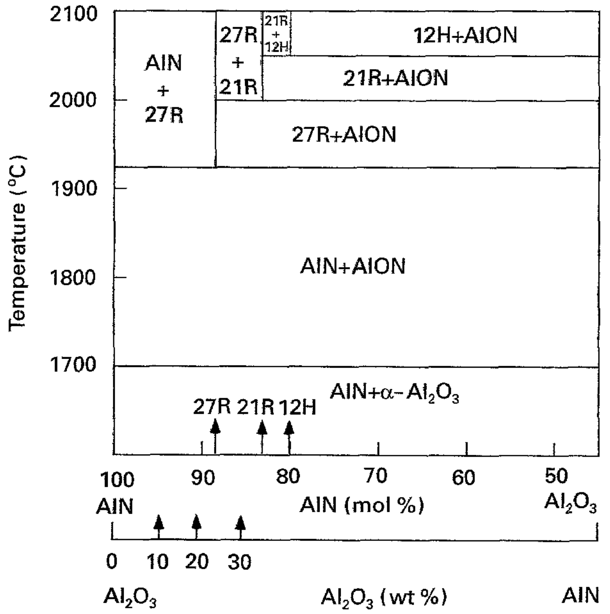

Figure 1 Phase diagram of the AlN–Al_2O_3 system.

2.2. Procedure

Each powder composition was blended in organic solvent for 6 h by wet ball milling with a plastic pot and Al_2O_3 balls. After drying, the granules were prepared through a 48 mesh sieve. The powder mixture was die-pressed into a pellet of 15 mm diameter × 5 mm under 100 MPa, and dewaxed at 600 °C in a nitrogen flow. Then the pellet was placed on BN jigs set in a graphite crucible in an electric furnace. According to the phase diagram given by McCauley and Corbin [11] shown in Fig. 1, the coexisting region of γ-AlON($5AlN \cdot 9Al_2O_3$) and 27R($7AlN \cdot Al_2O_3$) polytypoid is observable above 1920 °C. Thus the pellets were sintered at 1900° and 1950 °C for 6 h in 0.6 MPa nitrogen. A heating rate of 10 °C min^{-1} was applied. After firing, specimens were slowly cooled to room temperature in the furnace.

Phases present in the sintered specimen were analysed by X-ray diffraction (XRD, Rigaku RAD-R). Polished surfaces of the sintered specimens were used for the XRD measurement, and changes in crystal phase were compared in terms of relative intensities of peak height. The morphologies of fractured surfaces were observed by scanning electron microscopy (SEM, Jeol TSM-F7).

3. Results and discussion

3.1. Changes in phases present

3.1.1. AlN–Al_2O_3 system

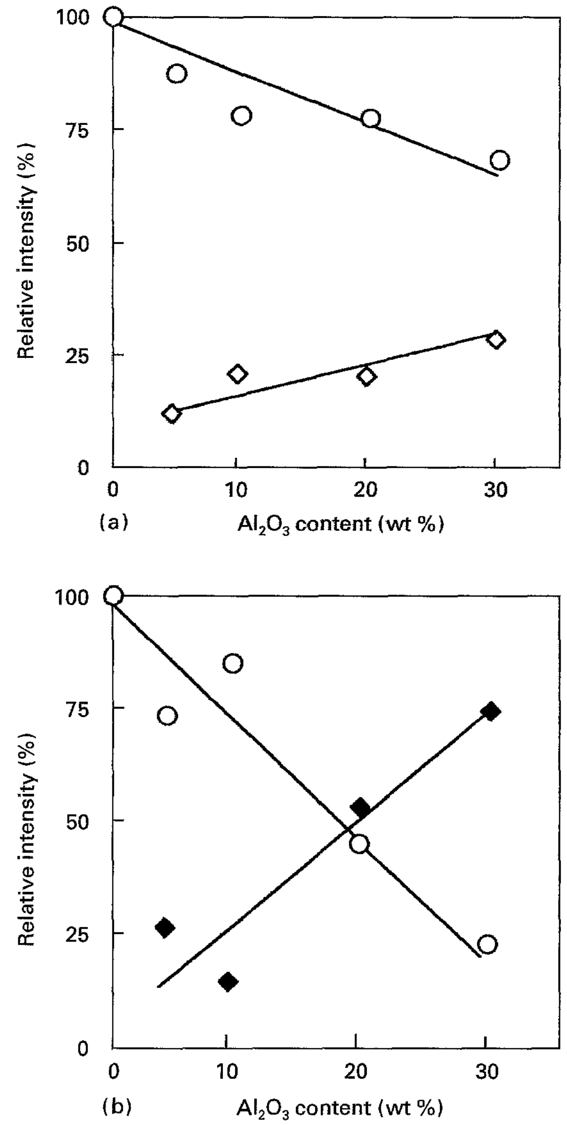

Figure 2 Changes in the phases present in sintered specimens. (a) 0 wt % Y_2O_3, 1900 °C, 6 h; (b) 0 wt % Y_2O_3, 1950 °C, 6 h. (○) AlN, (◇) γ-AlON, (◆) 27R.

The variations of phases present in sintered specimens with 0 wt % Y_2O_3 are shown in Fig. 2. The phases present fired at 1900 and 1950 °C were AlN and γ-AlON, AlN and 27R, respectively. Compared to the diagram given by McCauley and Corbin [11], the phases present in 1900 °C specimens are consistent, but those in 1950 °C specimens are inconsistent, with the diagram in that γ-AlON phase is not found in the Al_2O_3-rich region. As can be seen from Fig. 2, the amount of resultant γ-AlON in the specimen fired at 1900 °C sluggishly increases with increasing Al_2O_3 content, while in the specimens fired at 1950 °C, AlN phase decreases steeply and simultaneously 27R increases rapidly with increasing Al_2O_3 content. Incidentally, it is clear that the amount of AlN reacting with Al_2O_3 to form 27R at 1950 °C is much larger than that reacting to form γ-AlON at 1900 °C. Equations 1 and 2 indicate that the reason for this is because 1 mol Al_2O_3 reacts with 5/9 mol AlN to form 1/9 mol γ-AlON, and 1 mol Al_2O_3 requires 63/9 mol AlN to produce 1/9 mol 27R

$$5AlN + 9Al_2O_3 \rightarrow 5AlN \cdot 9Al_2O_3\ (\gamma\text{-AlON}) \quad (1)$$

$$7AlN + Al_2O_3 \rightarrow 7AlN \cdot Al_2O_3\ (27R) \quad (2)$$

Consideration with regard to the phase reaction will be described later.

3.1.2. AlN–Y_2O_3–Al_2O_3 system

Fig. 3 illustrates the phase changes in the sintered specimens with 3 wt % Y_2O_3. In the specimens with-

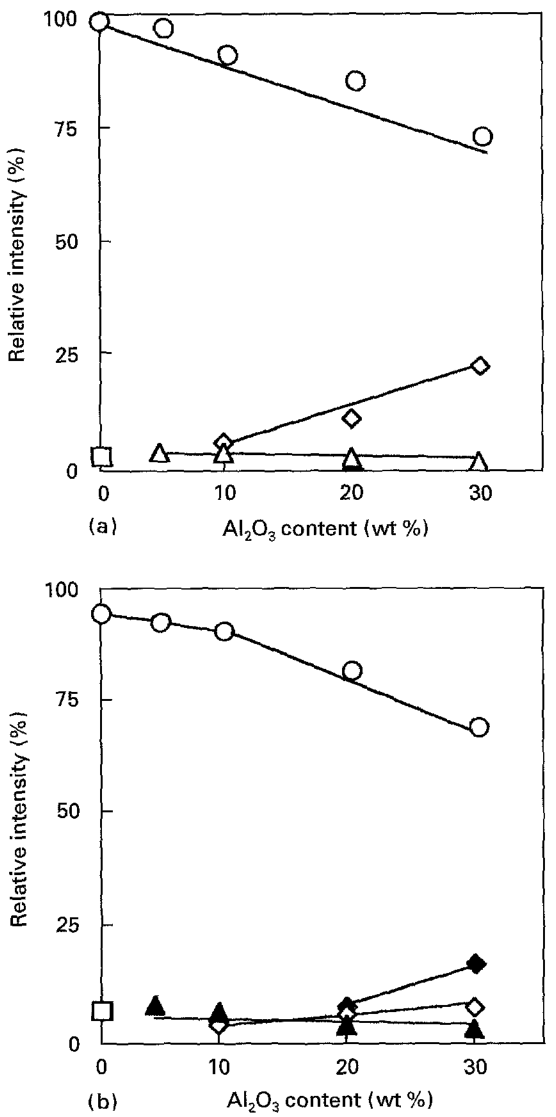

Figure 3 Changes in the phases present in sintered specimens. (a) 3 wt % Y_2O_3, 1900 °C, 6 h; (b) 3 wt % Y_2O_3, 1950 °C, 6 h. (○) AlN, (□) YAM, (△) YAG, (▲) YA, (◇) γ-AlON, (◆) 27R.

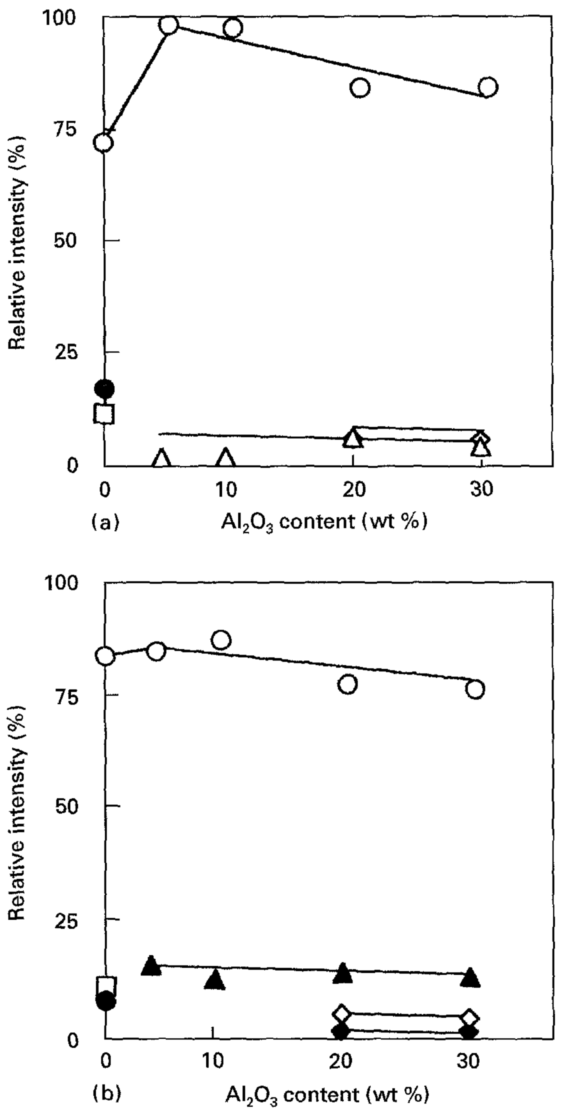

Figure 4 Changes in the phases present in sintered specimens. (a) 10 wt % Y_2O_3, 1900 °C, 6 h; (b) 10 wt % Y_2O_3, 1950 °C, 6 h. (○) AlN, (●) Y_2O_3, (□) YAM, (△) YAG, (▲) YA, (◇) γ-AlON, (◆) 27R.

out Al_2O_3, YAM($Al_2O_3 \cdot 2Y_2O_3$) phase is formed by the reaction of Y_2O_3 with Al_2O_3, from the surface of the AlN powder and from aluminium and oxygen in the bulk. In the system containing Al_2O_3 at 1900 °C, the phases are composed of AlN, YAG($5Al_2O_3 \cdot 3Y_2O_3$), and γ-AlON. In the relatively low concentration of 5 wt % Al_2O_3, γ-AlON phase is absent, and only YAG phase appears. In the Al_2O_3 rich region over 10 wt %, YAG and γ-AlON coexist, but an increase of Al_2O_3 content does not bring about the quantitative rise of YAG. This is considered to be because the initial amount of Y_2O_3 was small, so that the resulting YAG phase was limited, while the tendency for γ-AlON to increase with increasing Al_2O_3 is similar to the system without Y_2O_3.

In 1950 °C specimens with 3 wt % Y_2O_3, the phases are significantly different from the 1900 °C specimens. In all specimens with Al_2O_3, yttro-alumite (YA) which is a high-temperature type of YAG, is formed instead of YAG at 1950 °C. Moreover, phases present in the Al_2O_3-rich region over 20 wt % have 27R crystal. The existence of γ-AlON, as well as 1900 °C specimens, is recognized in the region from 10–30 wt % Al_2O_3. It is very interesting that γ-AlON, which has not been observed in the AlN–Al_2O_3, appears in the AlN–Y_2O_3–Al_2O_3 system.

Fig. 4 shows the changes of phases in sintered specimens with 10 wt % Y_2O_3. The phases in specimens without Al_2O_3 fired at both temperatures, are composed of AlN, YAM and Y_2O_3. The detection of Y_2O_3 implies that the amount of Y_2O_3 exceeds that required to yield YAM. The formation of YAG at 1900 °C and YA at 1950 °C is recognized as analogous to the result in Fig. 3. In the case of specimens containing 20 and 30 wt % Al_2O_3, γ-AlON and γ-AlON plus 27R are present at 1900 and 1950 °C, respectively. The phenomena of phase appearance are similar to the 3 wt % system, except that 27R decreases extremely. In any event, there is a great difference in phases between the AlN–Y_2O_3 and the AlN–Y_2O_3–Al_2O_3 as summarized in Table I. An additional experiment to confirm the phase-reaction process was conducted at both temperatures using such couples as YAG/AlN, YAG/γ-AlON and YAG/27R. The heating condition was applied corresponding to the description in the experimental section. After firing, the features in disc-type YAG set

TABLE I Phase reaction for the selected sintering conditions

Temp. (°C)	Comp. (wt %)	Phases present			
		γ-AlON $5AlN \cdot 9Al_2O_3$ (1.8)[a]	27R $7AlN \cdot Al_2O_3$ (0.14)	YAG $5Al_2O_3 \cdot 3Y_2O_3$ (1.7)	YA $5Al_2O_3 \cdot 3Y_2O_3$ (1.7)
1900	0Y20A[b]	+ + +[c]	–	–	–
	3Y20A	+ +	–	+	–
1950	0Y20A	–	+ + + +	–	–
	3Y20A	+ +	+ +	–	+

[a] Numbers in parentheses denote the molar ratio of Al_2O_3/AlN.
[b] Y,Y_2O_3(wt%); A,Al_2O_3(wt%).
[c] Intensity: + + + + > + + + > + + > +.

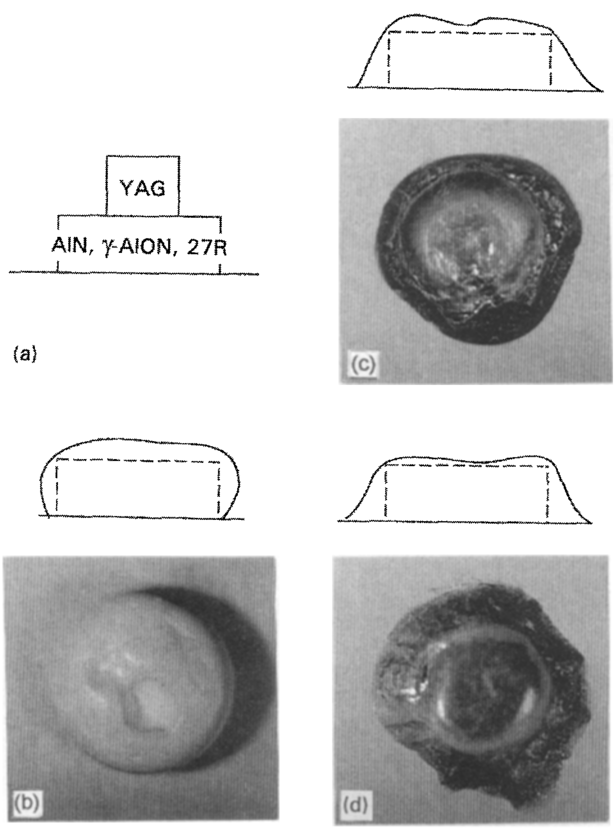

Figure 5 Features of various couples fired at 1950 °C: (a) before firing, (b) YAG/AlN, (c) YAG/γ-AlON, (d) YAG/27R.

on the discs of γ-AlON, 27R and AlN were observed. The size of YAG pellets was 10 mm diameter and 5 mm thick and those of the other components were 15 mm diameter and 4 mm thick. The couples fired at 1900 °C almost retained their original shape and separated easily with gentle force, indicating that no reaction took place at that temperature. On the contrary, the couples fired at 1950 °C retained no trace of their original form, as shown in Fig. 5. The order of the active reaction promotion was YAG/γ-AlON, YAG/27R and YAG/AlN. It was characteristic that the formation of bubbles in the couple of YAG/γ-AlON was clearly recognized, which seems to indicate that some volatile matter existed in this system. In the YAG/AlN and YAG/27R systems, no evolution was observed. A detailed analysis is currently being performed.

To investigate the effect of Al_2O_3 addition as to whether phase reaction is via a liquid phase, shrinkage rates of pellet-type specimens of AlN–10 wt % Y_2O_3 and AlN–10 wt % Y_2O_3–20 wt % Al_2O_3 were measured under 0.6 MPa nitrogen using a laser-beam device. The specimens were heated from room temperature to 1200 °C for 1 h, and then heated to 1950 °C for 1 h. The specimens were kept at 1950 °C for 30 min. Fig. 6 illustrates the shrinkage curves. It is recognized that the temperature at which shrinkage initiates for the AlN–Y_2O_3–Al_2O_3 specimen is approximately 1500 °C, which is about 250 °C lower than that for the AlN–Y_2O_3 specimen. This fact indicates that in the former system a liquid phase is produced at relatively lower temperatures. We suppose that the liquid phase is composed of the Y–Al–O compound. The solution of AlN into the liquid phase consisting of aluminate might be concerned with the phase reaction [16].

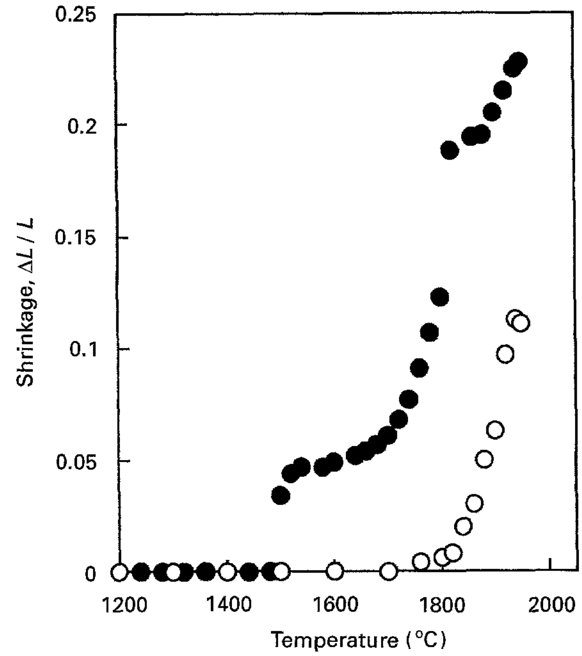

Figure 6 Shrinkage curves of pelletted specimens. (○) AlN–10 wt % Y_2O_3, (●) AlN–10 wt % Y_2O_3–20 wt % Al_2O_3 specimens.

3.2. Microstructures

Figs 7 and 8 show scanning electron micrographs of the fractured surfaces of the specimens sintered at 1900

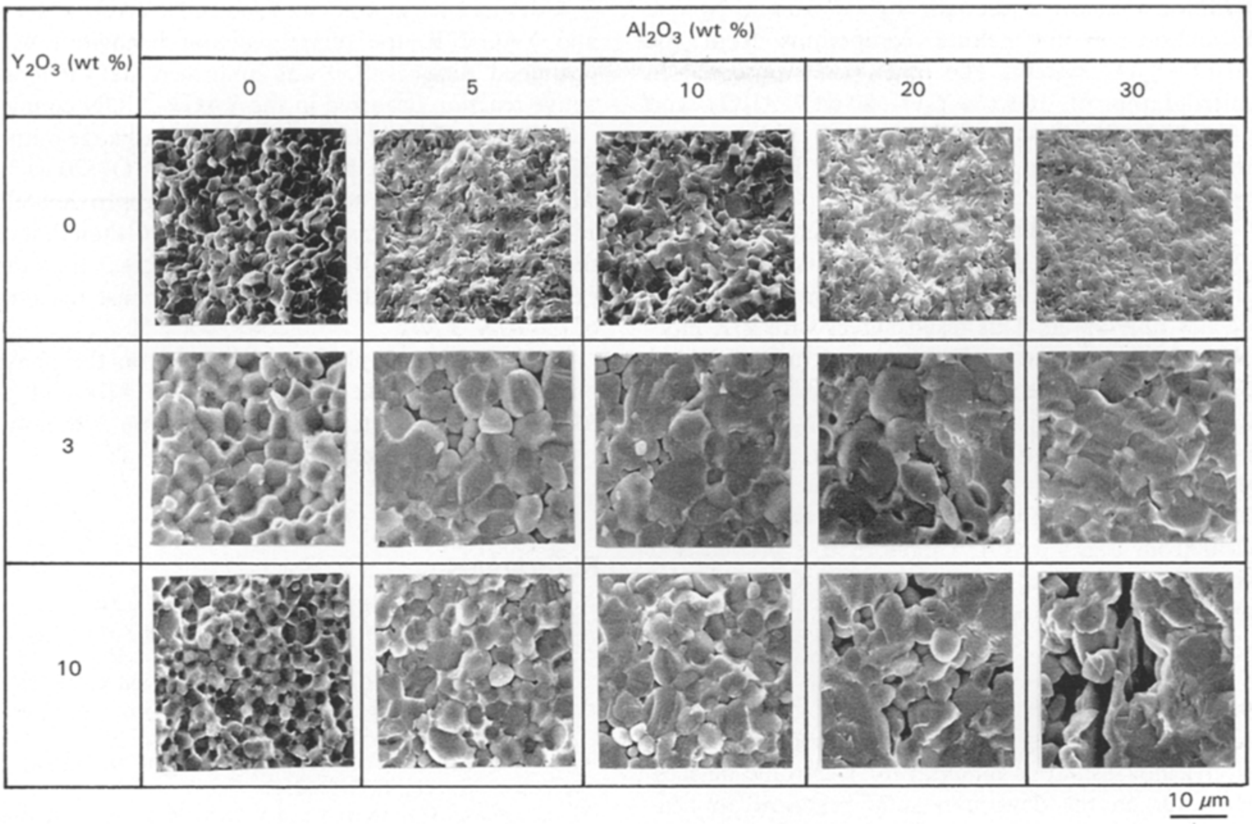

Figure 7 Scanning electron micrographs of fractured surfaces of the specimens sintered at 1900 °C for 6 h.

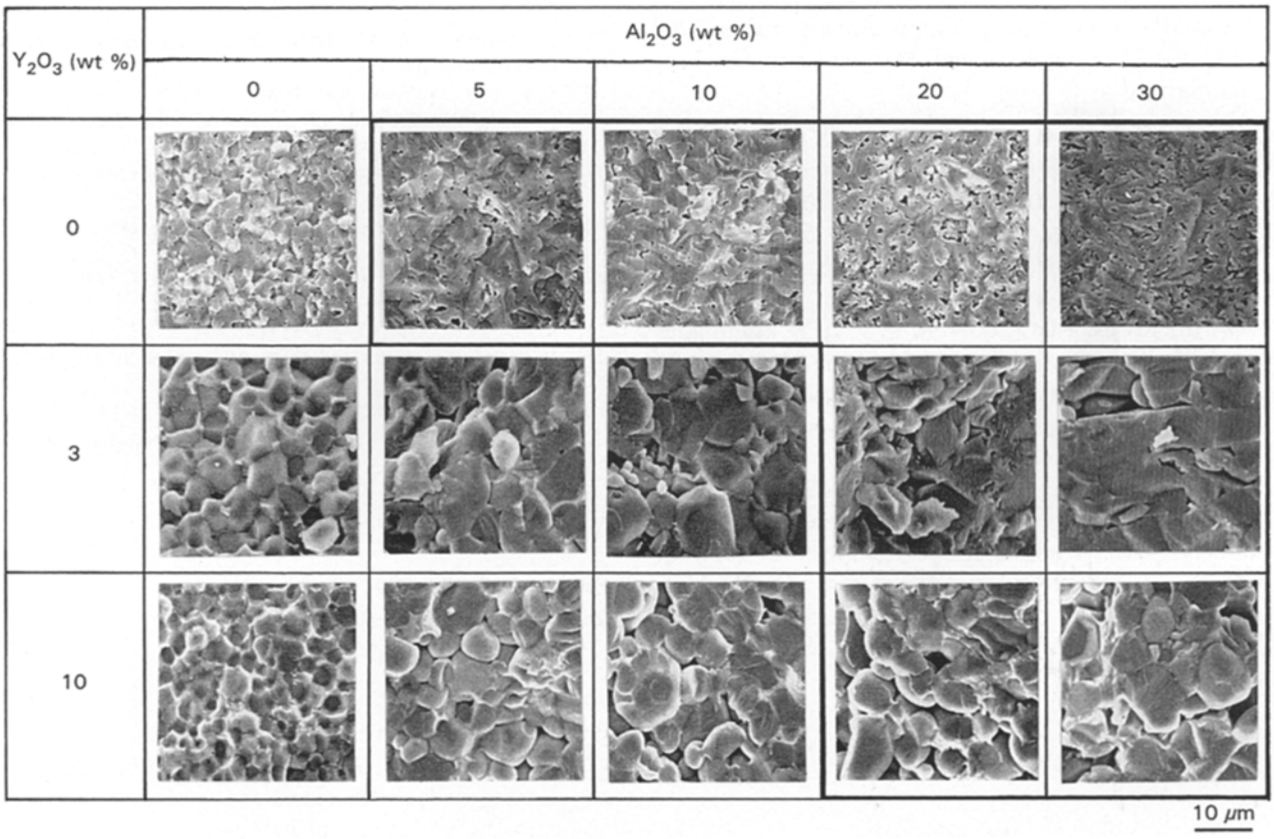

Figure 8 Scanning electron micrographs of fractured surfaces of the specimens sintered at 1950 °C for 6 h.

and 1950 °C, respectively. The grain morphologies in 1900 °C specimens are granular, which seems to be due to the crystal structure of AlN and γ-AlON grains. From these micrographs, it is proved that in the $AlN–Al_2O_3$ system, grain growth was disturbed with an increase in Al_2O_3, whereas in the $AlN–Y_2O_3–Al_2O_3$ system it is rather promoted by the Al_2O_3 addition. The grain-growth promotion in the Y_2O_3

addition system is thought to be caused by the formation of low-melting compounds from the Al_2O_3–Y_2O_3 system. The large pores observed in micrographs of 10 wt % Y_2O_3–20 wt % Al_2O_3 and 10 wt % Y_2O_3–30 wt % Al_2O_3 seem to originate from the volatilization of some species, as described previously.

On the other hand, in the specimens sintered at 1950 °C, it is found that the Al_2O_3 content is responsible for the plate-like grain-formation characteristic of 27R polytypoid. This result agrees with 27R morphology as reported by Komeya and Inoue [2] and Sakai [9]. As can be seen in Figure 8, plate-like grains are found in the region of higher Al_2O_3 content and lower Y_2O_3 content (encircled region). We suppose that the presence of Y_2O_3 controls the formation of 27R. The XRD analysis also supports the result as is clear from Figs 3 and 4. Therefore, it is proved that simultaneous addition of Y_2O_3 and Al_2O_3 sensitively affects the morphology.

4. Conclusions

AlN is a promising high-thermally conductive and electrically insulative material for electronic devices. However, in the development of practical applications, a critical problem is posed by the fact that the existence of oxygen in the AlN powders causes an extreme decrease of thermal conductivity. In this paper, the effect of Al_2O_3 addition on the phase reaction of the AlN–Y_2O_3 system at high temperatures of 1900 and 1950 °C was investigated. The results obtained are summarized as follows.

1. In the AlN–Al_2O_3 system, γ-AlON formation increased with increasing Al_2O_3 content at 1900 °C firing, while at 1950 °C, 27R polytypoid was formed, which is consistent with the phase diagram from McCauley and Corbin [11].
2. In the AlN–3 wt % Y_2O_3 system, YAM phase with the lowest Al_2O_3 content in yttrium aluminates was identified. On the other hand, in the AlN–10 wt % Y_2O_3 system, unreacted Y_2O_3 was detected in addition to YAM, because the Y_2O_3 was in excess of the amount required for the YAM yield.
3. The phase reaction in the AlN–Y_2O_3–Al_2O_3 system was quite different from that of the AlN–Al_2O_3: namely, γ-AlON and 27R coexisted even at 1950 °C, which is inconsistent with McCauley and Corbin's diagram [11].
4. Using such couples as YAG/AlN, YAG/γ-AlON and YAG/27R, the phase reaction behaviour was examined. As a result, it was confirmed that the most active reaction occurred in the YAG/γ-AlON couple.
5. By the dilatometric method, the shrinkage initiation temperature of the AlN–10 wt % Y_2O_3–20 wt % Al_2O_3 system was confirmed to be approximately 1500 °C, which was lower by about 250 °C than that of the AlN–10 wt % Y_2O_3. This fact suggests that the existence of Al_2O_3 strongly affects the phase reaction of the AlN–Y_2O_3.
6. The grain morphology depended on the phase present, in which the grains based on AlN and γ-AlON were granular, and those based on 27R polytypoid were plate-like.

References

1. G. A. SLACK, *J. Phys. Chem. Solids* **34** (1973) 321.
2. K. KOMEYA and H. INOUE, *Trans. J. Brit. Ceram. Soc.* **70** (1971) 107.
3. F. UENO, M. KASORI, A. HORIGUCHI and K. OHISHI, in "Annual Meeting of The Ceramic Society of Japan", preprint, Tokyo, April 1993, p. 1.
4. K. KOMEYA, T. TSUGE, H. INOUE and H. OHTA, *J. Mater. Sci. Lett.*, **1** (1982) 32.
5. K. KOMEYA, H. INOUE and A. TSUGE, *Yogyo-Kyokai-shi* **89** (1981) 330.
6. G. YAMAGUCHI and H. YANAGIDA, *J. Chem. Soc. Jpn* **32** (1959) 1264.
7. G. LONG and L. M. FOSTER, *J. Am. Ceram. Soc.* **44** (1961) 255.
8. I. ADAMS, I. R. AUCOIN and G. A. WOLFF, *J. Electrochem. Soc.* **109** (1962) 1050.
9. T. SAKAI, *Yogyo-Kyokai-Shi* **86** (1978) 125.
10. J. W. McCAULEY and N. D. CORBIN, *J. Am. Ceram. Soc.* **63** (1979) 476.
11. *Idem*, "Progress in Nitrogen Ceramics" (Boston Martinus Nijhoff, Boston, 1983) p. 111.
12. K. KOMEYA, H. INOUE and A. TSUGE, *J. Am. Ceram. Soc.* **57** (1974) 411.
13. L. J. GAUCKLER, H. L. LUKAS and G. PETZOW, *ibid.* **58** (1975) 346.
14. K. H. JACK, *J. Mater. Sci.* **11** (1976) 1135.
15. H. BUHR, G. MULLER and H. WIGGERS, *J. Am. Ceram. Soc.* **74** (1991) 718.
16. S. ARINAGA, K. SHINOZAKI, N. MIZUTANI, in "Annual Meeting of The Ceramic Society of Japan", preprint, Nagoya, April 1994, p. 349.

Received 16 May 1994
and accepted 8 September 1995